Transactions of the Materials Research Society of Japan 29[5] 1917-1920 (2004)

Development of segmented thermoelectric materials for high performance waste heat recovery and power generation devices

A.Yamamoto, T.Noguchi, H.Takazawa, C.H.Lee and H.Obara

National Institute of Advanced Industrial Science and Technology (AIST),
Umezono 1-1-1, AIST Central2, Tsukuba, Ibaraki, Japan
Fax: 81-29-861-5754, e-mail: a.yamamoto@aist.go.jp

Two stages segmented P-type and N-type thermoelectric materials have been developed. The P-type element consists of β-Zn_4Sb_3 and $(Bi_2Te_3)_{0.15}(Sb_2Te_3)_{0.85}$ and N-type consists of $CoSb_{2.85}Te_{0.15}$ and $(Bi_2Te_3)_{0.95}(Bi_2Se_3)_{0.05}$ targeting thermal-to-electrical conversion efficiency of 10% using waste heat around 700K. Calculation results on output power characteristics based on thermoelectric transport properties of individual materials revealed that the 4.2mm high PN unicouple is capable to produce 550mW electrical power at the efficiency of 10.5% if we correctly optimize their dimensions.

Key words: thermoelectric energy conversion, segmented element, Seebeck effect, waste heat recovery.

1. INTRODUCTION

Recent widespread trend in materials flow in our daily life, "less emissions, more reuse and recycle" is valid for an energy flow. Though a conversion efficiency of individual system has been enhanced continuously for several decades, both at demand side and at supply side, thermal energy has not been utilized effectively because of its low exergy compared to electricity or light. Vast energy is spoiled in a shape of low-grade thermal energy every day. Recovery and reuse of theses low-density, dispersed energy will help decreasing the fossil fuel consumption or suppressing CO_2 emission

Thermoelectric power generation (TEG) gives one of the practical solutions to utilize such useless low-grade waste heat by producing additional electrical power with a simple system, which uses no moving parts. Although application of TEG with radioactive heat source has been quite successful in space missions [1], there exists a cost or/and performance barrier to commercialize TEG in industrial and household sectors.

After a number of new findings of novel high performance thermoelectric materials in 1990's, it became easier to design power generation devices which possess conversion efficiency of η=10%-15%. Jet Propulsion Laboratory (JPL) has been making effort on integration of six different thermoelectric materials in one PN couple to maximize η up to 15% under temperature difference ΔT=973K[2,3]. New Energy and Industrial Technology Development Organization (NEDO) has started R&D program from 2002, targeting 12% and 15% thermoelectric energy conversion with segmented and cascaded materials under ΔT=550K[4].

We have tried to achieve 10% efficiency using β-Zn_4Sb_3 (β-ZS) and Bi-Sb-Te alloy (BST) for P-type and Te doped $CoSb_3$ (CST) and Bi-Te-Se alloy (BTS) for N-type. In this paper we report the thermoelectric properties of each materials and an experimental result of power generation characteristics of two stages segmented materials.

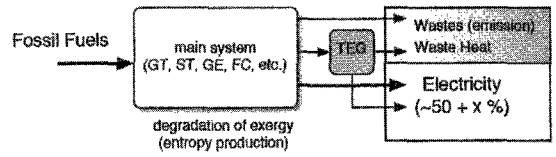

Fig. 1 A conceptual sketch of thermoelectric waste heat recovery applied to a conventional power generation system.

2. EXPERIMENTAL

2.1 Evaluation of individual materials parameters

All of the bulk materials discussed in this paper were prepared by powder metallurgy process using ball milling and uniaxial hot-pressing. The preparation parameters such as nominal composition of the materials, the solid reaction conditions, and the hot-pressing temperature had been tuned to maximize Z for each material prior to the experiment and summarized in Table I. The hot-pressed bulk pellet was cut into 3 x 3 x 15mm rectangular specimen to evaluate temperature dependence of the resistivity ρ and the Seebeck coefficient S in a temperature range from 310K to 700K. Thermal conductivity at room temperature was determined by steady-state relative method using 5 x 5 x 5mm quartz cube as a standard material. The thermal conductivity at elevated temperature was estimated using the electrical component calculated from Wiedemann-Franz low, where the Lorenz number is 2.45×10^{-8} (V^2/K^2) and the lattice component, which is assumed to be proportional to inverse T.

The thermal expansion coefficient of β-ZS, BST, and CST were also measured using above-mentioned rectangular specimen from 300K to 700K in argon atmosphere.

2.2 Preparation and evaluation of segmented materials

The uniaxial hot-press was also used for joining two different materials, i.e., β-ZS and BST for P-type; CST

Table I Hot-pressing conditions

	$(Bi_{0.15}Sb_{0.85})_2Te_3$	$Bi_2(Te_{0.95}Se_{0.05})_3$	$Co(Sb_{0.95}Te_{0.05})_3$	β-Zn_4Sb_3
duration	60 min.	60 min.	180 min.	480 min.
temp.	723K	723K	873K	743K
pressure	100 MPa	100 MPa	100 MPa	100 MPa

and BTS for N-type. We succeeded a coincident hot-pressing, where the two different powders were filled in a die simultaneously, for P-type materials. Because the process temperatures are quite different as seen in Table I for N-type, we tested two steps hot-pressing, where a bulk CST pellet and the powder BTS were set in the dies. The jointed materials were cut into 3.2 x 3.2 x 4.2mm, then tested power generation characteristics under large temperature difference around ΔT~350K. The thermoelectric output voltage V was picked up from electrical leads attached to two ends of the segmented material, and an external DC current source was connected to the material in series so that we can change the load current I as a parameter. The relation between V and I was plotted under several constant ΔT conditions.

3. RESULTS

3.1 Transport properties of thermoelectric materials

Fig. 1 (a), (b), (c) and (d) show the temperature dependence of Seebeck coefficient S, resistivity ρ, thermal conductivity κ, and figure of merit Z for all materials used in this study. BST and β-ZS had relatively better performance compared to BTS and CST. The resistivity of P-type materials is roughly two times larger than that of N-type, which means an element size optimization is necessary to equalize both internal resistances. The figure of merit Z and ZT of β-ZS was 1.4 x 10^{-3} K^{-1} and 0.94 at 660K and these values are 30% smaller than reported values [6]. We think that the difference comes from a difference in preparation process, but we should note that the data were quite reproducible and had practical mechanical strength, which is important for practical use. The Z value of BTS is rather low compared with conventional melt-grown materials since the process in this study cannot control anisotropy of the material.

3.2 Design of segmented structure.

Averaged figure of merit $\langle Z \rangle$ over the wide temperature range from 300K to 700K is defined as follows;

$$\langle Z \rangle = \frac{1}{700-300}\left(\int_{300}^{T_j} Z_1(T)\cdot dT + \int_{T_j}^{700} Z_2(T)\cdot dT\right) \quad (1)$$

where T_j is a temperature at the joint interface of two different thermoelectric materials. We determined the joint temperature T_j using curves shown in Fig.2 (d) to maximize the $\langle Z \rangle$. Thus calculated $\langle Z_p \rangle$ and $\langle Z_n \rangle$ are 1.87 x 10^{-3} K^{-1} for T_j=560K and 1.47 x 10^{-3} K^{-1} for T_j=590K, respectively. Considering T_j and the thermal

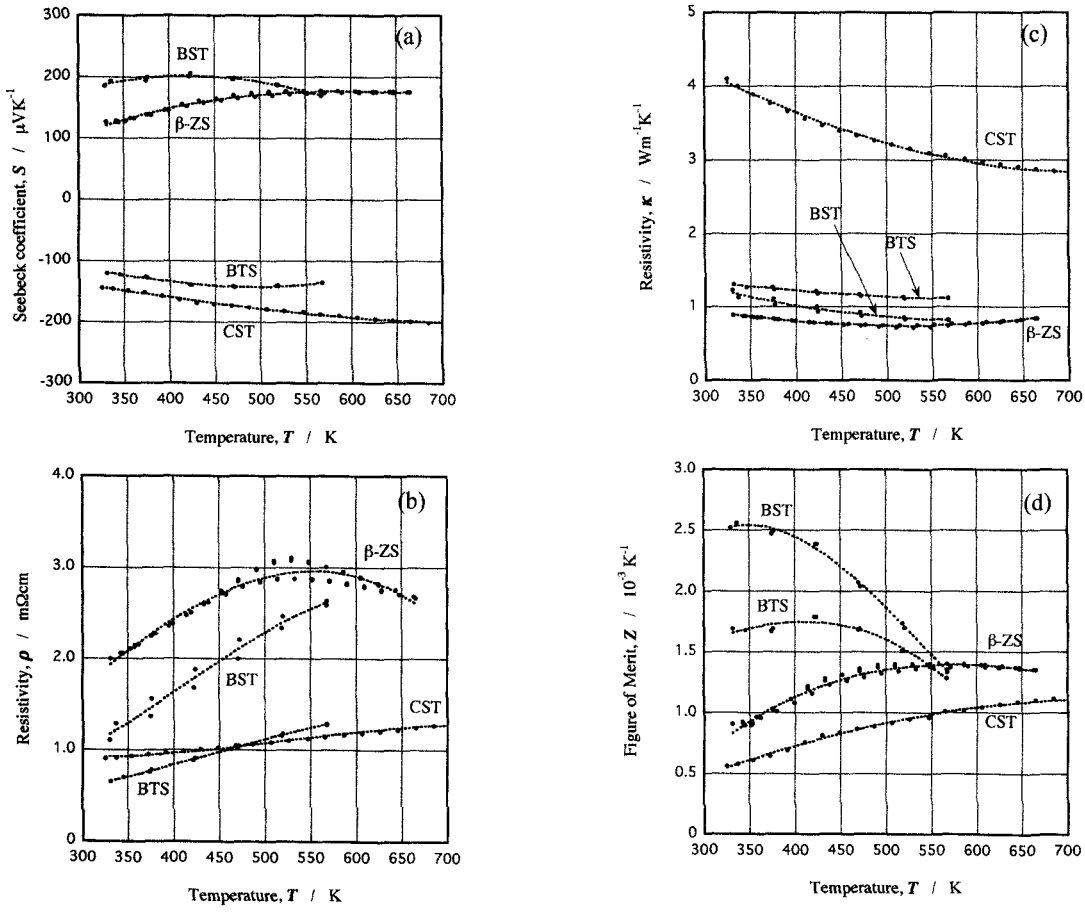

Fig.2 The temperature dependence of Seebeck coefficient S (a), electrical resistivity ρ (b), thermal conductivity κ (c) and figure of merit Z (d). The figure of merit Z were calculated value using $Z=S^2/(\rho\kappa)$.

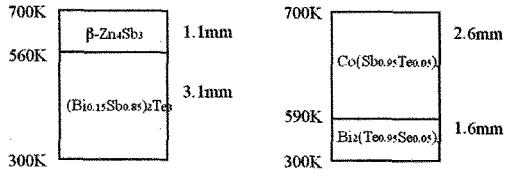

Cross-section : 3.2mm x 3.2mm Height : 4.2mm are given in this study.

Fig.3 Illustration of designed segmented structures.

conductivity of each material, the dimensions of segmented materials are designed as shown in Fig.3.

Power generation characteristics are estimated by numerical solution of differential equations listed below;

$$C\frac{dT}{dt} = STI - A\kappa\frac{dT}{dx} + I^2\rho\frac{dx}{A} \quad (2)$$

$$R = \frac{1}{A}\int_{x=0}^{x=L}\rho(x,T)dx \qquad V = \int_{T_{x=0}}^{T_{x=L}}S(x,T)dT \qquad I = \frac{V}{R+R_L} \quad (3)$$

$$\eta = \frac{P_{OUT}}{Q_{IN}} = \frac{Q_{IN}-Q_{OUT}}{Q_{IN}} \quad (4)$$

where C, R_L, A, η, P_{OUT}, Q_{IN}, Q_{OUT} are specific heat, external load resistance, cross-sectional area of the material, electrical power output, heat input, and heat output, respectively.

In the model for the numerical solution, the segmented material was divided into 100 cells and the parameter $S(T)$, $\rho(T)$ and $\kappa(T)$ were given as three-orders fitting curve taken from Fig.2 for each material.

Fig.4 shows calculated results of output power P_{out} and conversion efficiency η of P-type, N-type materials.

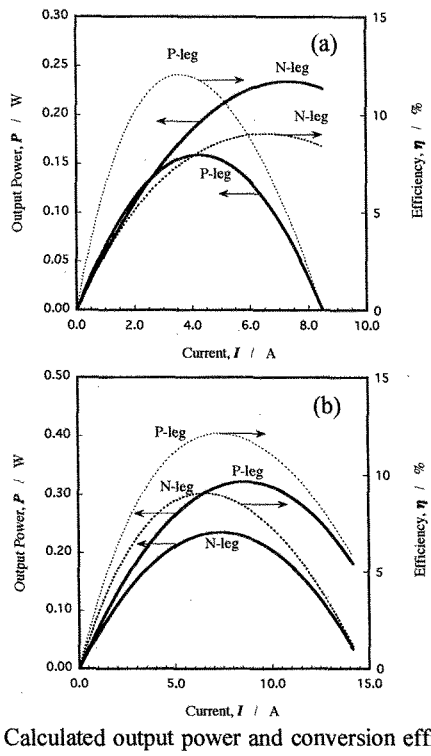

Fig.4 Calculated output power and conversion efficiency of two stage segmented P-type and N-type materials under ΔT=400K (a) : a case for the cross section area $A_P = A_N$, (b) : a case for $A_P = 2A_N$.

In the case of Fig.4 (a), the maxima of P_{out}=159mW and η=12.1% of P-leg appear at current I=4A, whereas those of N-type appear at I=7A. This is because of difference of the internal resistance. If the cross-section area of P-type material A_P is twice of that of N-type A_N, the current which gives maximum P_{out} becomes closer each other at I=7-8A, as shown in Fig.4 (b). The results of the model calculation are summarized in Table II. We find that we can expect the conversion efficiency larger than 10% for P-N single couple if we correctly prepare the segmentation structure as shown in Fig.3 and optimize the area of each materials, A_P and A_N.

Table II Estimated maximum output power and conversion efficiency at ΔT=400K.

element size of P-leg	P-leg		N-leg		P-N pair	
	P_{max} (mW)	η (%)	P_{max} (mW)	η (%)	P_{max} (mW)	η (%)
3.2 x 3.2 x 4.25	159	12.1	235	9.1	363	9.5
3.2 x 6.4 x 4.25	323	12.1	235	9.1	550	10.5

3.3 Power output characteristics

Pictures of two stages segmented materials prepared on the route of a coincident hot-pressing are shown in Fig.5. Through an optical microscope observation, we confirmed a trace of micro-crack both for the P-type and for N-type just after the slicing. We inserted a thin iron layer as a barrier layer to suppress interdiffusion between β-ZS and BST.

The segmented materials were cut into the designed dimensions, 3.2mm x 3.2mm, and then held between a heat source and a heat sink, which are controlled to keep a constant temperature to apply large ΔT to the materials.

Fig. 6 shows output characteristics of P-type and N-type segmented materials. The maximum output power was 115mW at ΔT=354K for P-type, and 118mW at ΔT=340 for N-type, respectively. The internal resistance of each segmented material was calculated from the slope of the V-I relation in Fig.6, and together with the open circuit thermoelectric voltage, summarized in Table III.

The open circuit voltage and the internal resistance of P-type element showed a good agreement with the calculated values based on the measured thermoelectric parameters for β-ZS and BST shown in Fig.2. On the other hand, the internal resistance of N-type was 36% larger than that of the calculated value. This increase of internal resistance was caused by micro-cracks in the vicinity of joint interfaces, which were observed after the power generation test.

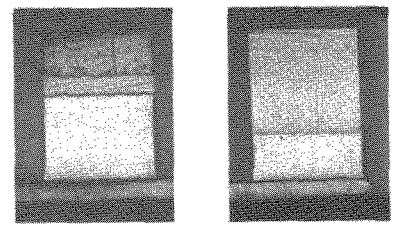

Fig.5 Optical microscope views of P-type (left) and N-type (right) segmented materials prepared by coincident hot-pressing. Dimensions : 3.2 x 3.2 x 4.2mm.

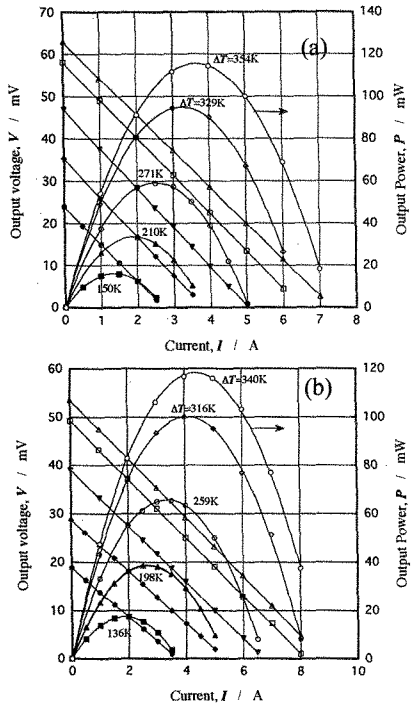

Fig.6 Experimental results of output voltage V and output power P of the segmented P-type (a) and N-type (b) materials, under ΔT=354K and ΔT=340K, respectively.

Table III Comparison between experimental results on power generating characteristics and corresponding calculated results.

P-leg						
	ΔT (K)	V_{oc} (mV)	I_{opt} (A)	P_{max} (mW)	R_{in} (mΩ)	η (%)
Experiment	354	62.9	3.69	115.4	8.58	--
Calculation	350	66.3	3.76	124.7	8.86	10.75
Ratio	101%	95%	98%	93%	97%	--

N-leg						
	ΔT (K)	V_{oc} (mV)	I_{opt} (A)	P_{max} (mW)	R_{in} (mΩ)	η (%)
Experiment	340	53.6	4.41	118.2	6.08	--
Calculation	350	55.7	6.25	177.6	4.48	7.82
Ratio	97%	96%	71%	67%	136%	--

4. DISCUSSIONS

The power generation characteristics of P-type segmented material showed a good agreement with calculated designed values, which means that the design of segmentation is quite successful. The increase of internal resistance in N-type material implies that the interface should be modified with some additional insert layers to reinforce mechanical strength. Measurements of thermal expansion coefficient revealed that there is a huge mismatch between CST and BTS, i.e. 7 x 10^{-6} K^{-1} and 18 x 10^{-6} K^{-1} at 300K. It seems necessary to introduce stress relaxation structure to realize a reliable interface in the case of CST/BTS combination.

The output power measurement in this study demonstrated that reasonable electrical power was produced using the segmented thermoelectric materials. 115mW under ΔT~350K for P-type material is equivalent to specific output power density of 2670mW/cm^3 or 405mW/g. Together with a conversion efficiency of 10%, these device specifications give us an image of quite promising future application. Especially TEG seems to match with small scale demand-side power generation systems such as Solid Oxide Fuel Cells, Micro-Turbine, and Gas-Engine system where the target power generation capability is several to several tens of kW, and the exhaust gas temperature is higher than 700K.

5. SUMMARY

We prepared segmented thermoelectric materials using uniaxial, coincident hot-pressing method. P-type consists of β-ZS and BST and N-type consists of CST and BTS. The optimized segmented structures were calculated for both P-type and N-type, using numerical iteration method. The model calculation revealed that the combination of above-mentioned materials with optimized structure possess 10.5% conversion efficiency under temperature difference of 400K.

V-I characteristics and output power were measured experimentally for both P-type and N-type material under the temperature difference of 350K. We confirmed that the segmentation of P-type materials was quite successful using iron layer for joint interface, whereas the N-type had a problem stemmed from a mismatch of the thermal expansion coefficients.

References

[1] D.M.Rowe ed., CRC Handbook of Thermoelectrics, CRC Press, 515-538 (1995)
[2] T. Caillat, J.-P. Fleurial, A. Borshchevsky, Phys. Chem. Solids **58**, 1119-1125(1997).
[3] T. Caillat, et al. Proc. Int. Conf. On Thermoelectrics, (1996)
[4] cf. NEDO homepage http://www.nedo.go.jp

(Received October 10, 2003; Accepted October 31, 2003)